



Blowing/suction effect on hydromagnetic heat transfer by mixed convection from an inclined continuously stretching surface with internal heat generation/absorption

Emad M. Abo-Eldahab *, Mohamed A. El Aziz

Department of Mathematics, Faculty of Science, Helwan University, P.O. Box 11795, Cairo, Egypt

Received 19 August 2003; received in revised form 26 December 2003; accepted 12 January 2004

Available online 9 April 2004

Abstract

The problem of steady, laminar, hydromagnetic heat transfer by mixed convection over a continuously stretching surface with power-law variation in the surface temperature or heat flux in the presence of internal heat generation/absorption effect is investigated. The surface velocity of the stretching surface was assumed to vary according to power-law. The surface is assumed to be permeable to allow for possible fluid wall blowing or suction. The governing non-similar equations are obtained by introducing a suitable transformation and are solved numerically. The obtained results are checked against previously published work on special cases of the problem and are found to be in excellent agreement. A parametric study is performed to illustrate the influence of the magnetic parameter, wall mass transfer coefficient, the coefficients of space-dependent and temperature-dependent internal heat generation/absorption, and the buoyancy force parameters on the fluid velocity and temperature profiles. Numerical data for the local skin-friction coefficient and the local Nusselt number have been tabulated for various parametric conditions.

© 2004 Elsevier SAS. All rights reserved.

1. Introduction

Boundary layer flow on continuous moving surfaces is an important type of flow occurring in a number of engineering processes. Aerodynamic extrusion of plastic sheets, cooling of an infinite metallic plate in a cooling path, which may be an electrolyte, crystal growing, the boundary layer along a liquid film in condensation processes and a polymer sheet or filament extruded continuously from a die, or along thread traveling between a feed roll and a wind-up roll are examples of practical applications of continuous moving surfaces. Glass blowing, continuous casting, and spinning of fibers also involve the flow due to a stretching surface. In 1961, Sakiadis [1,2] initiated the study of the boundary layer flow over a continuous solid surface moving with constant speed. Due to the entrainment of ambient fluid, this boundary layer flow situation is quite different from the classical Blasius problem of boundary flow over a semi-infinite flat plate. Erickson et al. [3] extended the work of Sakiadis to account for mass transfer at the stretched sheet surface.

Tsou et al. [4] reported both analytical and experimental results for the flow and heat transfer aspects developed by a continuously moving surface. Soundalgekar and Ramana Murthy [5] investigated the constant surface velocity case with a power-law temperature variation. There are several practical applications in which significant temperature differences between the surface of the body and the ambient fluid exist. These temperature differences cause density gradients in the fluid medium and in the presence of gravitational body force, free convection effects become important. A situation where both the forced-and free-convection are of comparable order is called mixed convection. The friction factor and heat transfer rate can be quite different under mixed convection conditions relative forced convection case. Karwe and Jaluria [6] showed that the thermal buoyancy effects are more prominent when the plate moves vertically. Ingham [7] investigated the existence of the solution for the free convection boundary layer flow near a continuously moving vertical plate with temperature inversely proportional to the distance up the plate. Mixed convection arises in many transport processes in natural and engineering devices (such as atmospheric boundary layer flow, heat exchangers, solar collector, nuclear reactors, and electronic equipment).

* Corresponding author.

E-mail address: e_aboeldahab@hotmail.com (E.M. Abo-Eldahab).

Nomenclature

A, B, C	prescribed constants	Re_x	local Reynolds number
A^*	space-dependent internal heat generation/absorption	T	fluid temperature
B^*	temperature-dependent internal heat generation/absorption	T_w	wall temperature of the moving sheet
B_0	magnetic induction	T_∞	ambient temperature
C_{fx}	local friction coefficient	u	velocity of the fluid in the x -direction
c_p	specific heat at constant pressure	u_w	velocity of the moving sheet
f	dimensionless stream function for the PST case	v	velocity of the fluid in the y -direction
f_w	dimensionless suction/blowing parameter	V_w	surface mass flux x - and y -directions, respectively
F	dimensionless stream function for the PHF case	x, y	axial and normal coordinates
C	concentration	<i>Greek symbols</i>	
C_{fx}	local skin friction coefficient	α	thermal diffusivity
g	acceleration due to gravity	β	coefficient of thermal expansion
h	local heat transfer coefficient	η	dimensionless normal distance
Gr_x	local Grashof number PST case	θ	dimensionless temperature for the PST case
Gr_x^*	modified local Grashof number PHF case	μ	dynamic viscosity
k	thermal conductivity	ν	kinematic viscosity
m	heat flux exponent parameter	ξ	buoyancy force parameter for the PST case
M	magnetic parameter	ρ	density
n	temperature exponent parameter	ζ	buoyancy force parameter for the PHF case
Nu_x	local Nusselt number	τ_w	local skin friction
p	velocity exponent parameter	ϕ	dimensionless temperature for the PHF case
Pr	Prandtl number	σ	electric conductivity
q'''	rate of internal heat generation or absorption	ψ	stream function
q_w	surface heat flux		

Ali and Al-Yousef [8] have reported the problem of laminar mixed convection adjacent to a uniformly moving vertical plate with suction or injection. Recently, Chen [9] treated the mixed convection heat transfer from a vertical continuously stretching sheet. All the above investigations are restricted to a continuous surface moving with constant velocity which is not adequate for many practical applications. Since the surface undergoes stretching and cooling or heating that cause surface velocity and temperature variations. Danberg et al. [10] investigated the non-similar solution for the flow in the boundary layer past a wall that is stretched with a velocity proportional to the distance along the wall. Vlegaar [11] studied the momentum and heat transfer to a continuous, accelerating surface by assuming linear variation of surface velocity with respect to distance from the slot. Groubka and Bobba [12] analyzed the stretching problem for surface moving with a linear velocity and with variable surface temperature. Ali [13] has reported flow and heat transfer characteristics on a stretched surface subjected to power-law velocity and temperature distributions. The flow field of a stretching wall with a power-law velocity variation was investigated by Banks [14]. Recently, Ali [15] and El-bashbeshy [16] extended Banks work for a porous stretched surface for different values of the injection parameter. All the above investigations are restricted to hydrodynamic flow

and heat transfer problems. However, of late, hydromagnetic flows and heat transfer have become more important in recent years because of many important applications. For example, many metallurgical processes which involve cooling of continuous strips or filaments, these elements are drawn through a quiescent fluid. During this process, these strips are sometimes stretched. The properties of the final product depend to a great extent on the rate of cooling. This rate of cooling and therefore, the desired properties of the end product can be controlled by the use of electrically conducting fluids and the application of the magnetic fields [17]. The use of magnetic fields has been also used in the process of purification of molten metals from non-metallic inclusions. Many works have been reported on flow and heat transfer of electrically conducting fluids over a stretched surface in the presence of magnetic field (see for instance, Chakrabarti and Gupta [18], Chiam [19] and Chandran et al. [20], Subhas et al. [21]). In several practical applications, there exist significant temperature differences between the surface and the ambient fluid. This necessitates the consideration of temperature-dependent heat sources or sinks which may exert strong influence on the heat transfer characteristics (Vajravelu and Nayfeh [22]). The study of heat generation or absorption effects is important in view of several physical problems such fluids undergoing exothermic or endothermic

chemical reactions (Vajravelu and Hadjinicalaou [23]). Although, exact modeling of internal heat generation or absorption is quite difficult, some simple mathematical models can express its average behavior for most physical situations. Heat generation or absorption has been assumed to be constant, space-dependent or temperature-dependent. Crepeau and Clarksean [24] have used a space-dependent exponentially decaying heat generation or absorption in their work on flow and heat transfer from a vertical plate. Subhas et al. [25] studied the boundary layer flow and heat transfer of a visco-elastic fluid immersed in a porous medium over a non-isothermal stretching sheet in the presence of temperature-dependent heat source. Vajravelu and Hadjinicalaou [17] have considered hydromagnetic convective heat transfer from a stretching surface with uniform free stream and in the presence of temperature-dependent heat generation or absorption. Recently, Abo-Eldahab and El Gendy [26] extended the work of Vajravelu and Hadjinicalaou [17] to include the radiation and variable viscosity effects. Even more recently, Abo-Eldahab [27] analyzed the problem of free convection heat transfer due to the simultaneous action of buoyancy, radiation and transverse magnetic field near an isothermal stretching sheet in the presence of temperature-dependent heat generation or absorption. In the present work we have analyzed the mixed convection boundary layer flow of an electrically conducting fluid over an inclined continuously stretching surface with power-law variation in the surface temperature or heat flux in the presence of magnetic, internal heat generation/absorption, and wall suction/blowing effects.

2. Analysis

Consider a steady, laminar, hydromagnetic heat transfer by mixed convection flow along a continuous stretching semi-infinite sheet that is inclined from the vertical with an acute angle γ and situated in an otherwise quiescent ambient fluid at temperature T_∞ . The surface is assumed to be permeable and moving with power-law velocity, $u_w(x) = Cx^p$ (where C and p are constants). The x -axis runs along the continuous surface in the direction of motion with the slot as the origin and the y -axis is measured normally from the sheet to the fluid. A magnetic field of variable strength is applied normal to the sheet in the y -direction which produces magnetic effect in the x -direction (see Fig. 1). This is done in this way so as to allow suppression of convective flow in that direction. This is important in terms of controlling the quality of the product being stretched (see [17]). Two conditions at the surface considered in the analysis are (I) prescribed surface temperature (PST), $T_w(x) - T_\infty = Ax^n$ and (II) prescribed heat flux (PHF), $q_w(x) = Bx^m$. Here $T_w(x)$ and $q_w(x)$ are, respectively, temperature and heat flux at the wall; T_∞ is the temperature at large distance from the surface. A and B are dimensional constants, and m and n are exponents. In addition, the fluid

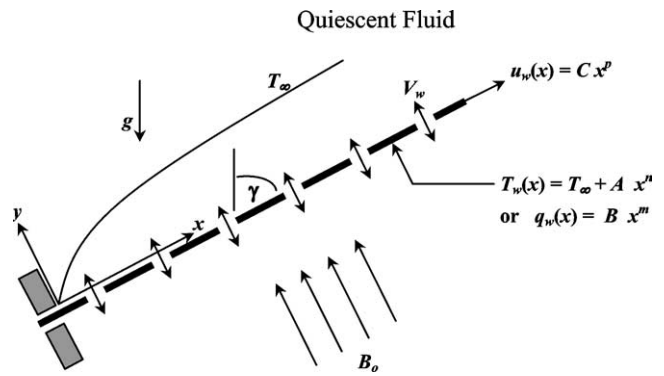


Fig. 1. Physical model and coordinates.

suction or blowing is imposed at the sheet surface in the y -direction. The fluid is assumed to be Newtonian, electrically conducting, heat generating or absorbing and has a constant properties except the density in the buoyancy term of the momentum equation. The magnetic Reynolds number of the flow is taken to be small enough so that the induced distortion of the applied magnetic field can be neglected. In addition, there is no applied electric field and the Hall effect, Joule heating and viscous dissipation are all neglected in this work. With the usual boundary layer and Boussinesq approximations the problem is governed by the following equations:

$$\frac{\partial u}{\partial x} + \frac{\partial v}{\partial y} = 0 \tag{1}$$

$$u \frac{\partial u}{\partial x} + v \frac{\partial u}{\partial y} = v \frac{\partial^2 u}{\partial y^2} \pm g\beta(T - T_\infty) - \frac{\sigma B_0^2}{\rho} u \tag{2}$$

$$\rho c_p \left(u \frac{\partial T}{\partial x} + v \frac{\partial T}{\partial y} \right) = k \frac{\partial^2 T}{\partial y^2} + q''' \tag{3}$$

where u, v and T are the fluid x -component of velocity, y -component of velocity and the temperature, respectively. ρ, ν, σ, k and c_p are the fluid density, kinematic viscosity, electrical conductivity, thermal conductivity, and specific heat at constant pressure of the fluid, respectively. β, q''', g and B_0 are the coefficient of thermal expansion, rate of internal heat generation (> 0) or absorption (< 0) coefficient, acceleration due gravity and magnetic induction, respectively. The plus and minus signs that appear on the right-hand side of Eq. (2) pertain to assisting and opposing flows respectively.

The internal heat generation or absorption term q''' is modeled according to the following equation:

$$q''' = \left(\frac{ku_w(x)}{x\nu} \right) [A^*(T_w - T_\infty)e^{-\eta} + B^*(T - T_\infty)] \tag{4}$$

where A^* and B^* are coefficients of space-dependent and temperature-dependent internal heat generation/absorption, respectively. In Eq. (4), the first term represents the dependence of the internal heat generation or absorption on the

space coordinates while the latter term represents its dependence on the temperature. Note that when both $A^* > 0$ and $B^* > 0$, this case corresponds to internal heat generation while for both $A^* < 0$ and $B^* < 0$, the case corresponds to internal heat absorption.

The boundary conditions suggested by the physics of the problem are:

$$\begin{aligned} u_w(x) &= Cx^p, & v &= V_w, & T_w(x) &= T_\infty + Ax^n & \text{or} \\ -k(\partial T/\partial y) &= q_w(x) = Bx^m & \text{at } y &= 0 \\ u &\rightarrow 0, & T &\rightarrow T_\infty & \text{as } y &\rightarrow \infty \end{aligned} \quad (5)$$

where V_w is the surface mass flux. It should be noted that positive values of V_w indicate fluid blowing at the sheet surface while negative values of V_w correspond to fluid suction at the wall.

Case (I): Prescribed surface temperature (PST),
 $T_w(x) - T_\infty = Ax^n$

We introduce the dimensionless variables

$$\begin{aligned} \eta &= (y/x)Re_x^{1/2} \\ \xi &= Gr_x \cos \gamma / Re_x^2 \\ f(\xi, \eta) &= \psi(x, y) / (vRe_x^{1/2}) \\ \theta(\xi, \eta) &= (T - T_\infty) / [T_w(x) - T_\infty] \end{aligned} \quad (6)$$

where $Re_x = u_w(x)x/\nu$ is the local Reynolds number; $Gr_x = g\beta[T_w(x) - T_\infty]x^3/\nu^2$ is the local Grashof number and $f(\xi, \eta)$ is the stream function satisfying the continuity equation with $u = \partial\psi/\partial y$ and $v = -\partial\psi/\partial x$. Eqs. (2) and (3) under the transformation (6) reduce to

$$\begin{aligned} f''' + \frac{1}{2}(p+1)ff'' - pf'^2 \pm \xi\theta - Mf' \\ = (n-2p+1)\xi \left(f' \frac{\partial f'}{\partial \xi} - f'' \frac{\partial f}{\partial \xi} \right) \end{aligned} \quad (7)$$

$$\begin{aligned} \theta'' + \frac{1}{2}(p+1)Prf'\theta' - nPrf'\theta + A^*e^{-\eta} + B^*\theta \\ = Pr(n-2p+1)\xi \left(f' \frac{\partial \theta}{\partial \xi} - \theta' \frac{\partial f}{\partial \xi} \right) \end{aligned} \quad (8)$$

The primes indicate differentiation with respect to η , $M = \sigma B_0^2 x / \rho u_w$ is the magnetic parameter and $Pr = \nu/\alpha$ is the Prandtl number of the fluid.

The transformed boundary conditions are given by:

$$\begin{aligned} f'(\xi, 0) &= 1, & f(\xi, 0) &= [2/(p+1)]f_w \\ \theta(\xi, 0) &= 1, & f'(\xi, \infty) &= 0, & \theta(\xi, \infty) &= 0 \end{aligned} \quad (9)$$

where $f_w = -(xV_w/\nu)Re_x^{-1/2}$ is the dimensionless suction/blowing parameter.

The local skin friction is given by:

$$\tau_{wx} = \mu \frac{\partial u}{\partial y} \Big|_{y=0} = \frac{\mu u_w Re_x^{1/2}}{x} f''(\xi, 0) \quad (10)$$

The local skin friction coefficients C_{fx} is defined as:

$$\begin{aligned} C_{fx} &= \frac{\tau_{wx}}{1/2\rho u_w^2(x)} = 2Re_x^{-1/2} f''(\xi, 0) & \text{or} \\ C_{fx} Re_x^{1/2} &= 2f''(\xi, 0) \end{aligned} \quad (11)$$

The local heat flux is given by

$$\begin{aligned} q_w(x) &= -k \frac{\partial T}{\partial y} \Big|_{y=0} \\ &= -\frac{k[T_w(x) - T_\infty] Re_x^{1/2}}{x} \theta'(\xi, 0) \end{aligned} \quad (12)$$

The local heat transfer coefficient may be written as follows,

$$h(x) = \frac{q_w(x)}{[T_w(x) - T_\infty]} = -\frac{k Re_x^{1/2}}{x} \theta'(\xi, 0) \quad (13)$$

The local Nusselt number is given by

$$\begin{aligned} Nu_x &= \frac{xh(x)}{k} = -Re_x^{1/2} \theta'(\xi, 0) & \text{or} \\ Nu_x Re_x^{-1/2} &= -\theta'(\xi, 0) \end{aligned} \quad (14)$$

Case (II): Prescribed heat flux (PHF), $q_w(x) = Bx^m$

For this case, the following non-similarity variables are invoked

$$\begin{aligned} \eta &= (y/x)Re_x^{1/2} \\ \zeta &= Gr_x^* \cos \gamma / Re_x^{5/2} \\ F(\zeta, \eta) &= \psi(x, y) / (vRe_x^{1/2}) \\ \phi(\zeta, \eta) &= (T - T_\infty) Re_x^{1/2} / [xq_w(x)/k] \end{aligned} \quad (15)$$

where $Gr_x^* = g\beta q_w(x)x^4/k\nu^2$ is the modified local Grashof number. Substitution of Eq. (15) into Eqs. (2)–(4) gives

$$\begin{aligned} F''' + \frac{1}{2}(p+1)FF'' - pF'^2 \pm \zeta\theta - MF' \\ = \frac{1}{2}(2m-5p+3)\zeta \left(F' \frac{\partial F'}{\partial \zeta} - F'' \frac{\partial F}{\partial \zeta} \right) \end{aligned} \quad (16)$$

$$\begin{aligned} \phi'' + \frac{1}{2}(p+1)PrF\phi' - \frac{1}{2}(2m-p+1)PrF'\phi \\ + A^*e^{-\eta} + B^*\phi(\zeta, 0) \\ = \frac{1}{2}Pr(2m-5p+3)\zeta \left(F' \frac{\partial \phi}{\partial \zeta} - \phi' \frac{\partial F}{\partial \zeta} \right) \end{aligned} \quad (17)$$

$$\begin{aligned} F'(\zeta, 0) &= 1, & F(\zeta, 0) &= [2/(p+1)]f_w \\ \phi'(\zeta, 0) &= -1 \\ F'(\zeta, \infty) &= 0, & \phi(\zeta, \infty) &= 0 \end{aligned} \quad (18)$$

The local skin friction coefficients C_{fx} is defined as:

$$C_{fx} Re_x^{1/2} = 2F''(\zeta, 0) \quad (19)$$

The local Nusselt number for this case is given by

$$Nu_x Re_x^{-1/2} = 1/\phi(\zeta, 0) \quad (20)$$

Table 1

Comparison of the values of $Nu_x Re_x^{-1/2}$ for various values of Pr with $M = f_w = A^* = B^* = p = n = 0$

Pr	Tsou et al. [4]	Soundagekar and Murty [5]	Jacobi [28]	Ali [15]	Present study
0.7	0.3492	0.3508	0.3492	0.3476	0.3497589
1.0	0.4438	–	0.4438	0.4416	0.4437779
10.0	1.6804	1.6808	1.6790	1.6713	1.6802900

Table 2

Comparison of the values of $-\theta''(0)$ for various values of Pr with $p = 1$ and $M = f_w = A^* = B^* = n = 0$

Pr	f_w	Gupta and Gupta [29]	Grubka and Bubba [12]	Lashmishka et al. [30]	Ali [15]	Present study
0.7	0	–	–	0.45446	–0.45255	–0.454449
1.0	0	–0.5820	–0.5820	–	–0.59988	–0.58201
10.0	0	–	–2.3080	–	–2.29589	–2.30801
1.0	–1.067	–0.1105	–	–	0.10996	–0.11077

Table 3

Comparison of $Nu_x Re_x^{-1/2}$ values with those of Ali for various values of Pr, f_w, n and p with $M = A^* = B^* = 0$

Pr	f_w	n	p	Ali [15]	Present study
0.72	0.2	–1.0	–0.2	–0.5568877	–0.55542938860827
0.72	0.4	–1.0	–0.2	–1.912207	–0.18985462183429
0.72	0.2	1.0	–0.2	0.8794258	0.88185620374677
0.72	0.2	–1.0	1.0	0.1410325	0.14299964764059
1.0	0.2	–1.0	–0.2	–0.7518967	–0.74928605671757
1.0	0.4	–1.0	–0.2	–0.2119652	–0.21093000324587
1.0	0.2	1.0	–0.2	1.0834070	1.09122129536463
1.0	0.2	–1.0	1.0	0.1969407	0.20000141468394
3.0	0.2	–1.0	–0.2	–1.6422180	–1.61132473587556
3.0	0.4	–1.0	–0.2	0.0858079	0.09077213201068
3.0	0.2	1.0	–0.2	2.1327440	2.14937409233131
3.0	0.2	–1.0	1.0	0.5929329	0.60001883784485
10.0	0.2	–1.0	–0.2	–1.2264180	–1.19955664480529
10.0	0.4	–1.0	–0.2	2.5606010	2.58357768276728
10.0	0.2	1.0	–0.2	4.5640030	4.60514886103890
10.0	0.2	–1.0	1.0	1.9848080	1.99996133394711

3. Results and discussion

The transformed Eqs. (7) and (8) subject to the boundary conditions (9) for PST case and Eqs. (16) and (17) with the boundary conditions (18) for PHF case are approximated by a system of non-linear ordinary differential equations replacing the derivatives with respect to ξ (PST case) and ζ (PHF case) by two-point backward finite difference with step size 0.01. These equations are integrated by fifth order Runge–Kutta–Fehlberg scheme with a modified version of the Newton–Raphson shooting method. In order to verify the accuracy of our present method, we have shown a comparison of our results for the values of $Nu_x Re_x^{-1/2}$ with those reported by Tsou et al. [4], Soundagekar and Murthy [5], Jacobi [28] and Ali [15] for forced convection flow on a continuous iso-thermal sheet ($n = 0$) with uniform motion ($p = 0$) (see Table 1). Also, Table 2 shows a comparison of the present results for the temperature gradient $-\theta''(0)$ with those reported by Gupta and Gupta [29], Grubka and

Bubba [12], Lashmishka et al. [30] and Ali [15] for $p = 1$ (linearly stretching surface), $n = 0$ (iso-thermal sheet) and various values of Prandtl number and suction/blowing parameter in the absence of magnetic field ($M = 0$), heat source/sink ($A^* = B^* = 0$). Table 3 illustrates the comparison of $Nu_x Re_x^{-1/2}$ values with those of Ali [15] for various values of Pr, f_w, n and p with $M = A^* = B^* = 0$. Finally, direct comparisons with the numerical results of $Nu_x Re_x^{-1/2}$ reported earlier by Ali [15] and Elbashbeshy [16] corresponding to uniform and variable surface heat flux are listed in Table 4 for various values of Pr, f_w, m and p with $M = A^* = B^* = 0$. In all cases, the results are found to be in good agreement. Our numerical values of $C_{fx} Re_x^{1/2}$ and $Nu_x Re_x^{-1/2}$ in PST and PHF cases are listed in Table 5 and 6, respectively.

The results of the numerical computations are displayed in Figs. 2–11 for prescribed surface temperature (PST) case and in Figs. 12–21 for prescribed heat flux (PHF) for dis-

Table 4
Comparison of $Nu_x Re_x^{-1/2}$ values with those of Ali for various values of Pr, f_w, n and p with $M = A^* = B^* = 0$

Pr	f_w	m	p	Ali [15]	Elbasheshy [16]	Present study
0.72	0.6	0.0	-0.2	0.8635	0.87280	0.86356408592001
0.72	0.6	1.0	-0.2	-	1.2010	1.18925269089293
0.72	-0.2	0.0	-0.2	0.6259	0.63090	0.62612301498750
0.72	-0.2	1.0	-0.2	-	1.0207	1.01363252786789
0.72	0.6	0.0	1.0	0.7623	0.77110	0.76218556391223
0.72	0.6	1.0	1.0	-	1.053	1.04192426434574
0.72	0.6	-1.0	1.0	-	0.4385	0.43201323586849
1.0	0.6	0.0	-0.2	1.1184	1.11800	1.11835169561874
1.0	0.6	1.0	-0.2	-	1.5022	1.50232914983100
1.0	-0.2	0.0	-0.2	0.7405	0.74090	0.74060700423775
1.0	-0.2	1.0	-0.2	-	1.1942	1.19420145005988
1.0	0.6	0.0	1.0	1.0063	1.00600	1.00616685528390
1.0	0.6	1.0	1.0	-	1.3437	1.34403078886055
1.0	0.6	-1.0	1.0	-	0.6	0.60000078214705
10.0	0.6	0.0	-0.2	7.2116	7.20330	7.21059816831847
10.0	0.6	1.0	-0.2	-	8.1824	8.18988791749153
10.0	-0.2	0.0	-0.2	1.8884	1.88840	1.88845492779472
10.0	-0.2	1.0	-0.2	-	3.2854	3.28574052708426
10.0	0.6	0.0	1.0	7.0923	7.09210	7.09207029523932
10.0	0.6	1.0	1.0	-	8.0128	8.01757210529307
10.0	0.6	-1.0	1.0	-	5.9988	6.00006280590303

Table 5
 $C_{f_x} Re_x^{1/2}$ and $Nu_x Re_x^{-1/2}$ for various values of M, f_w, A^* and B^* with $\xi = 0.5, p = 0.5, n = 0.5$ (PST)

M	f_w	A^*	B^*	ξ	$C_{f_x} Re_x^{1/2}$	$Nu_x Re_x^{-1/2}$
0.5	0.0	0.01	0.01	0.5	-1.52500621244659	0.60907667978284
1.0	0.0	0.01	0.01	0.5	-1.99060471723572	0.56892547701583
1.5	0.0	0.01	0.01	0.5	-2.39032311386178	0.53584605508042
0.1	-0.2	0.01	0.01	0.5	-0.89961378857639	0.58270085517066
0.1	-0.1	0.01	0.01	0.5	-0.98645429521673	0.61471620029534
0.1	0.0	0.01	0.01	0.5	-1.07999032665349	0.64832271400903
0.1	0.2	0.01	0.01	0.5	-1.28740762653015	0.72035480589573
0.1	0.6	0.01	0.01	0.5	-1.78222806101549	0.88370856255241
0.1	1.0	0.01	0.01	0.5	-2.37289952315999	1.07166909278642
0.1	0.0	-0.5	0.01	0.5	-1.20173754272619	0.99805188775280
0.1	0.0	-0.2	0.01	0.5	-1.12927975447412	0.79591834435538
0.1	0.0	0.0	0.01	0.5	-1.08565781850009	0.66340836831748
0.1	0.0	0.5	0.01	0.5	-0.98477636040447	0.33714304813358
0.1	0.0	1.0	0.01	0.5	-0.89263996416234	0.01654318714547
0.1	0.0	1.5	0.01	0.5	-0.80659869699309	-0.29968623628381
0.1	0.0	2.0	0.01	0.5	-0.72522519460674	-0.61232091374630
0.1	0.0	0.01	-0.4	0.5	-1.17638885848853	0.93242239415524
0.1	0.0	0.01	-0.2	0.5	-1.13987737852436	0.81098530219547
0.1	0.0	0.01	0.0	0.5	-1.09116578937478	0.66542145912908
0.1	0.0	0.01	0.1	0.5	-1.03348475579231	0.55076047067905
0.1	0.0	0.01	0.2	0.5	-0.98021066553650	0.44728612403509
0.1	0.0	0.01	0.01	0.0	-1.663611983231295	0.57811274074708
0.1	0.0	0.01	0.01	0.1	-1.536445938408255	0.59796759423584
0.1	0.0	0.01	0.01	0.2	-1.416133896069302	0.61348749568023
0.1	0.0	0.01	0.01	0.3	-1.300620663157744	0.62656821632244
0.1	0.0	0.01	0.01	0.4	-1.188803048817354	0.63803179730044
0.1	0.0	0.01	0.01	0.5	-1.079990326653494	0.64832271400907

tribution of the velocity and temperature fields. Results are obtained for $Pr = 0.7$ (air), $p = n = 0.5, m = 0$ and various values of the magnetic field parameter M , coefficient

of space-dependent internal heat generation/absorption A^* , coefficient of temperature-dependent internal heat generation/absorption B^* , suction/blowing parameter f_w and the

Table 6
 $C_{f_x} Re_x^{1/2}$ and $Nu_x Re_x^{-1/2}$ for various values of M , f_w , A^* and B^* with $\zeta = 0.5$, $p = 0.5$, $m = 0$ (PHF)

M	f_w	A^*	B^*	ζ	$C_{f_x} Re_x^{1/2}$	$Nu_x Re_x^{-1/2}$
0.5	0.0	0.01	0.01	0.5	-1.01050814455179	0.53993832691679
1.0	0.0	0.01	0.01	0.5	-1.45262932811317	0.50790815629029
1.5	0.0	0.01	0.01	0.5	-1.83522659995818	0.48167720882017
0.1	-0.4	0.01	0.01	0.5	-0.02846292652197	0.44913078691074
0.1	-0.2	0.01	0.01	0.5	-0.29484412589923	0.50541899007635
0.1	0.0	0.01	0.01	0.5	-0.59305839107939	0.57137573563285
0.1	0.2	0.01	0.01	0.5	-0.90531695236547	0.64265131593808
0.1	0.6	0.01	0.01	0.5	-1.58760630529800	0.80664107974279
0.1	1.0	0.01	0.01	0.5	-2.33073994376171	0.99873780066043
0.1	0.0	-0.6	0.01	0.5	-1.18686896745145	0.98922161566798
0.1	0.0	-0.3	0.01	0.5	-0.95922971474019	0.78140433581203
0.1	0.0	0.0	0.01	0.5	-0.62682882021669	0.58593813748006
0.1	0.0	0.3	0.01	0.5	-0.02751551113844	0.39570697856955
0.1	0.0	0.5	0.01	0.5	0.57481724798404	0.29163471436475
0.1	0.0	1.0	0.01	0.5	3.51723590558761	0.11729313707379
0.1	0.0	0.01	-0.6	0.5	-1.15623838365404	0.97117038064421
0.1	0.0	0.01	-0.3	0.5	-0.98864656863792	0.80016353699294
0.1	0.0	0.01	0.0	0.5	-0.62682882085576	0.58593813738934
0.1	0.0	0.01	0.3	0.5	0.57228278080601	0.30389841322629
0.1	0.0	0.01	0.5	0.5	2.58980577378259	0.15573713246644
0.1	0.0	0.01	0.01	0.0	-1.663611983231295	0.47883214117668
0.1	0.0	0.01	0.01	0.1	-1.393579965200941	0.50958620426580
0.1	0.0	0.01	0.01	0.2	-1.165596714893527	0.53027394036989
0.1	0.0	0.01	0.01	0.3	-0.960595731300540	0.54638161685317
0.1	0.0	0.01	0.01	0.4	-0.771070819453500	0.55978636472584
0.1	0.0	0.01	0.01	0.5	-0.593058391079394	0.57137573563284

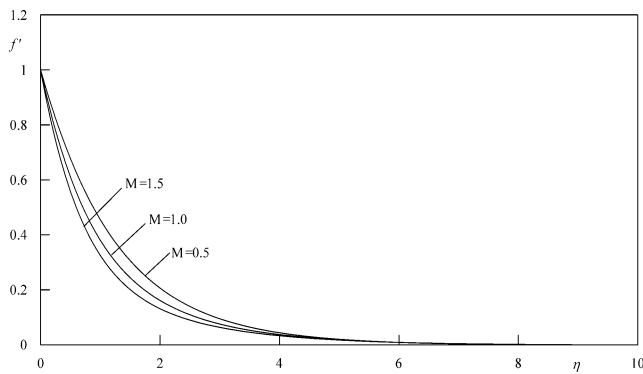


Fig. 2. Velocity profiles for various values of M with $A^* = 0.01$, $B^* = 0.01$, $f_w = 0$, $p = 0.5$, $n = 0.5$, $\xi = 0.5$ and $Pr = 0.7$, PST case.

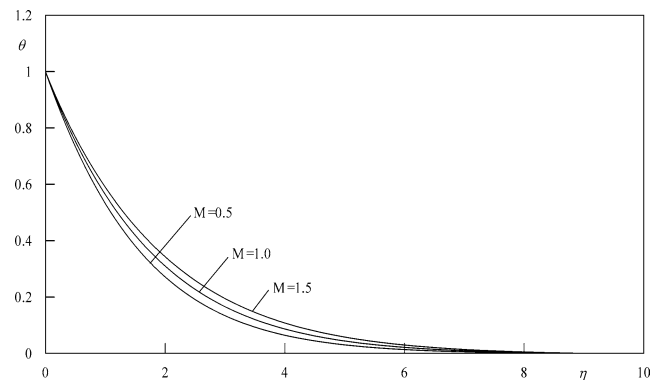


Fig. 3. Temperature profiles for various values of M with $A^* = 0.01$, $B^* = 0.01$, $f_w = 0$, $p = 0.5$, $n = 0.5$, $\xi = 0.5$ and $Pr = 0.7$, PST case.

buoyancy force parameters (ξ for the PST case and ζ for the PHF case). It is observed that these parameters affect the velocity and temperature fields. Figs. 2 and 3 present the behavior of the velocity f' and temperature θ profiles for various values of the magnetic parameter M . The presence of magnetic field in an electrically conducting fluid tends to produce a body force against the flow. This type of resistive force tends to slow down the motion of the fluid in the boundary layer which, in turn, reduces the rate of heat convection in the flow and this appears in increasing the flow temperature. Also, the effects on the flow and thermal fields become more so as the strength of the magnetic field in-

creases as shown in Figs. 2 and 3. Table 5 shows that, the local Nusselt number $Nu_x Re_x^{-1/2}$ and the local friction coefficient $C_{f_x} Re_x^{1/2}$ are both decreased with increasing the values of magnetic parameter M .

The influence of the presence of spatial-dependent internal heat generation ($A^* > 0$) or absorption ($A^* < 0$) in the boundary layer on the velocity and temperature fields are presented in Figs. 4 and 5, respectively. It is clear from these figures that increasing the values of A^* produces increases in the velocity and temperature distributions of the fluid. This is expected since the presence of heat source ($A^* > 0$) in the boundary layer generates energy which causes the tem-

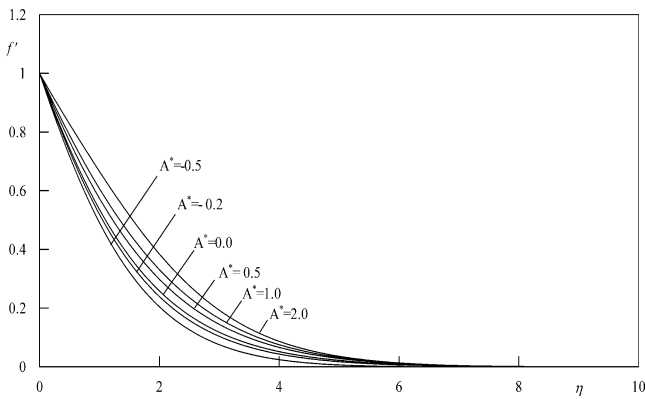


Fig. 4. Velocity profiles for various values of A^* with $M = 0.1, B^* = 0.01, f_w = 0, p = 0.5, n = 0.5, \xi = 0.5$ and $Pr = 0.7$, PST case.

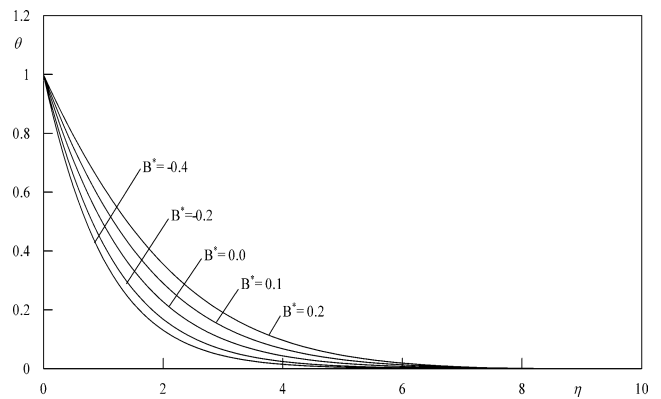


Fig. 7. Temperature profiles for various values of B^* with $M = 0.1, A^* = 0.01, f_w = 0, p = 0.5, n = 0.5, \xi = 0.5$ and $Pr = 0.7$, PST case.

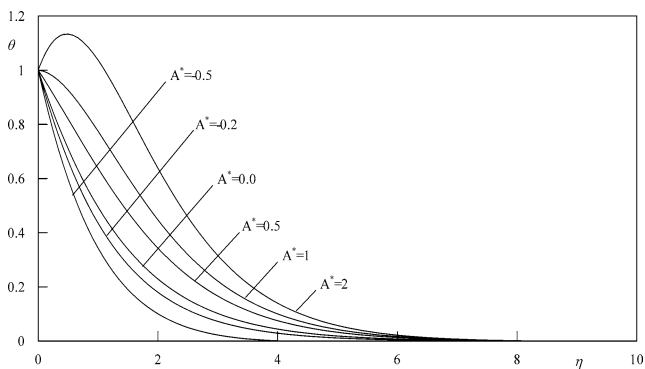


Fig. 5. Temperature profiles for various values of A^* with $M = 0.1, B^* = 0.01, f_w = 0, p = 0.5, n = 0.5, \xi = 0.5$ and $Pr = 0.7$, PST case.

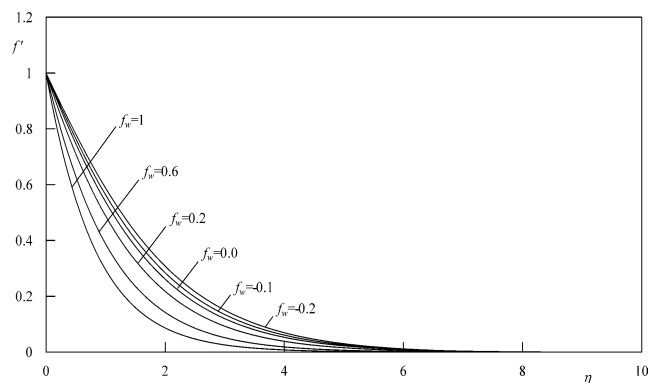


Fig. 8. Velocity profiles for various values of f_w with $M = 0.1, A^* = 0.01, p = 0.5, n = 0.5, \xi = 0.5$ and $Pr = 0.7$, PST case.

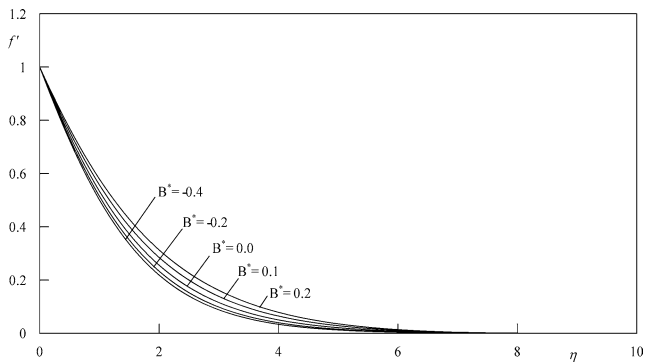


Fig. 6. Velocity profiles for various values of B^* with $M = 0.1, A^* = 0.01, f_w = 0, p = 0.5, n = 0.5, \xi = 0.5$ and $Pr = 0.7$, PST case.

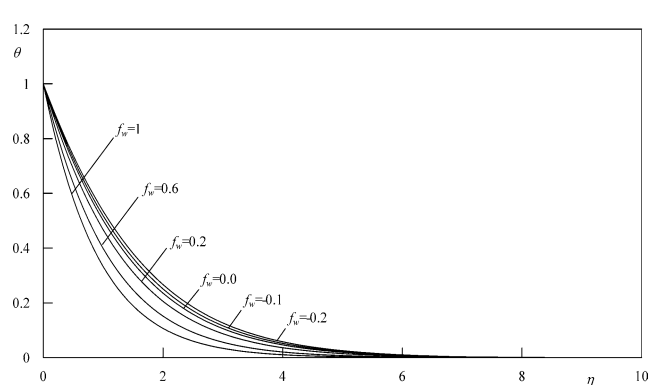


Fig. 9. Temperature profiles for various values of f_w with $M = 0.1, B^* = 0.01, p = 0.5, n = 0.5, \xi = 0.5$ and $Pr = 0.7$, PST case.

perature of the fluid to increase. This increase in the temperature produces an increase in the flow field due to the buoyancy effect. However, as the heat source effect get large ($A^* = 2$), a distinctive peak in the temperature profile occurs in the fluid adjacent to the wall. This means that the temperature of the fluid near the sheet higher than the sheet temperature and consequently, heat is expected to transfer to the wall. On the contrary, heat sink ($A^* < 0$) has the opposite effect, namely cooling of the fluid, reducing the flow velocity in the boundary layer as a result of the thermal buoy-

any effect which couples the flow and thermal problems. These behaviors are depicted in Figs. 4 and 5. Moreover, as shown from Table 5, as A^* increases, the local Nusselt number decreases while the local friction coefficient increases. It is noted that the negative heat transfer rates are obtained for higher values of A^* (e.g., $A^* = 1.5$ and 2). Negative values of $Nu_x Re_x^{-1/2}$ indicate that heat is transferred from the fluid to the moving surface as discussed before. The influence of the temperature-dependent internal heat generation ($B^* > 0$) or absorption ($B^* < 0$) in the boundary

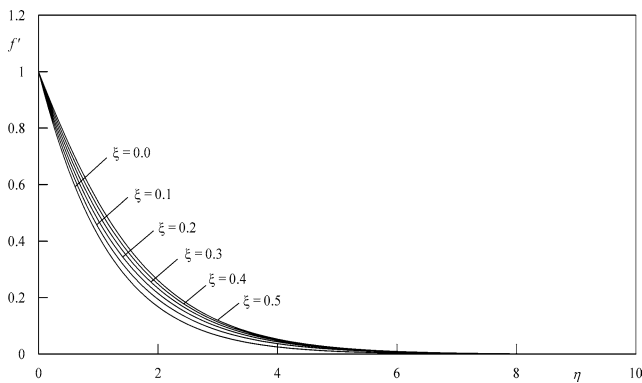


Fig. 10. Velocity profiles for various values of ξ with $M = 0.1$, $A^* = 0.01$, $B^* = 0.01$, $f_w = 0$, $p = 0.5$, $n = 0.5$ and $Pr = 0.7$, PST case.

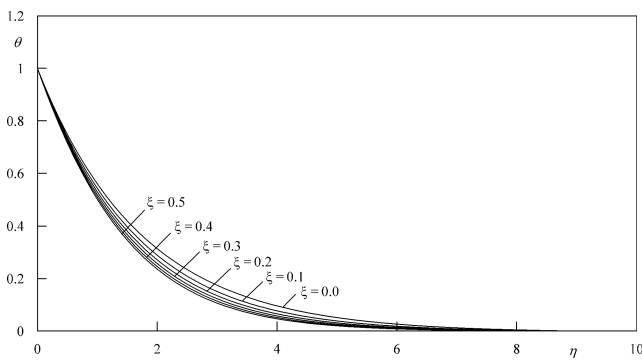


Fig. 11. Temperature profiles for various values of ξ with $M = 0.1$, $A^* = 0.01$, $B^* = 0.01$, $f_w = 0$, $p = 0.5$, $n = 0.5$ and $Pr = 0.7$, PST case.

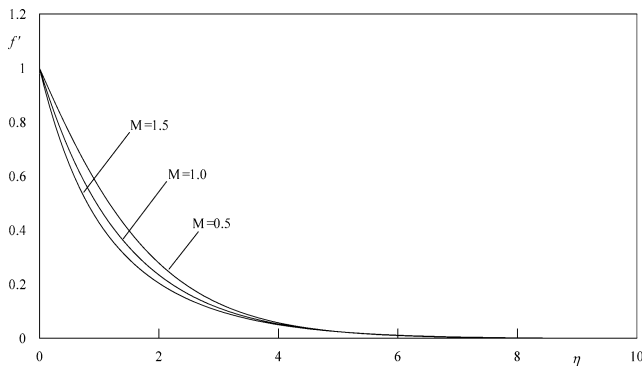


Fig. 12. Velocity profiles for various values of M with $A^* = 0.01$, $B^* = 0.01$, $f_w = 0$, $m = 0.0$, $p = 0.5$, $n = 0.5$, $\xi = 0.5$ and $Pr = 0.7$, PHF case.

layer on the flow and temperature fields is the same as that of spatial-dependent internal heat generation or absorption. Namely, for $B^* > 0$ (heat source), the velocity and temperature of the fluid increase while they decrease for $B^* < 0$ (heat sink). These behaviors are depicted in Figs. 6 and 7. Also, the local Nusselt number $Nu_x Re_x^{-1/2}$ decreases while the local friction coefficient $C_{f,x} Re_x^{1/2}$ increases due to an increase in the temperature-dependent internal heat generation/absorption B^* .

Figs. 8 and 9 depict the influence of the suction/blowing parameter f_w on the velocity and temperature profiles in

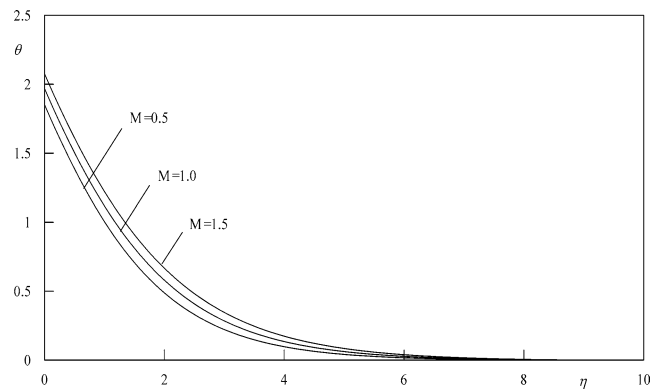


Fig. 13. Temperature profiles for various values of M with $A^* = 0.01$, $B^* = 0.01$, $f_w = 0$, $m = 0.0$, $p = 0.5$, $\xi = 0.5$ and $Pr = 0.7$, PHF case.

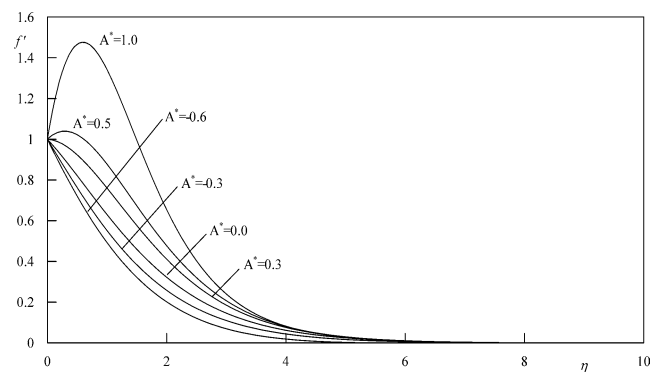


Fig. 14. Velocity profiles for various values of A^* with $M = 0.1$, $B^* = 0.01$, $f_w = 0$, $m = 0.0$, $p = 0.5$, $\xi = 0.5$ and $Pr = 0.7$, PHF case.

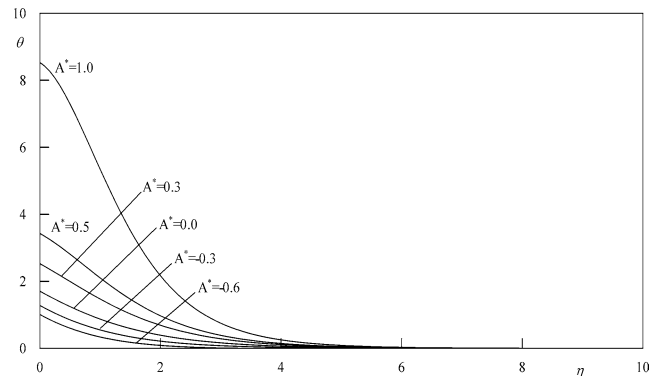


Fig. 15. Temperature profiles for various values of A^* with $M = 0.1$, $B^* = 0.01$, $f_w = 0$, $m = 0.0$, $p = 0.5$, $\xi = 0.5$ and $Pr = 0.7$, PHF case.

the boundary layer, respectively. It is known that imposition of the wall suction ($f_w > 0$) have the tendency to reduce both the momentum and thermal boundary layer thickness. This causes reduction in both the velocity and temperature profiles. However, the exact opposite behavior is produced by imposition of the wall fluid blowing or injection ($f_w < 0$). These behaviors are obvious from Figs. 8 and 9. Further, the results in Table 4 indicate that the dimensionless heat transfer coefficient $Nu_x Re_x^{-1/2}$ increases markedly with increasing suction and decreases with increasing in-

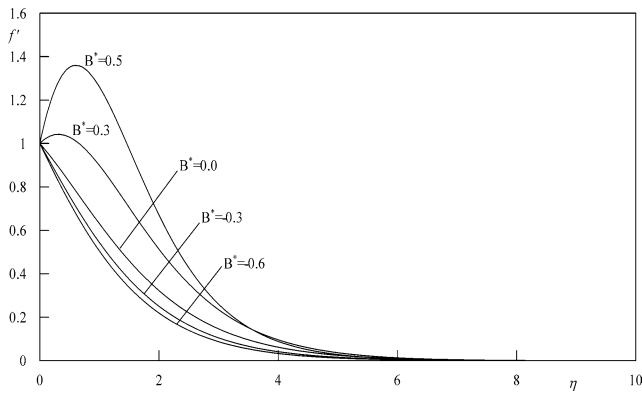


Fig. 16. Velocity profiles for various values of B^* with $M = 0.1$, $A^* = 0.01$, $f_w = 0$, $m = 0.0$, $p = 0.5$, $\zeta = 0.5$ and $Pr = 0.7$, PHF case.

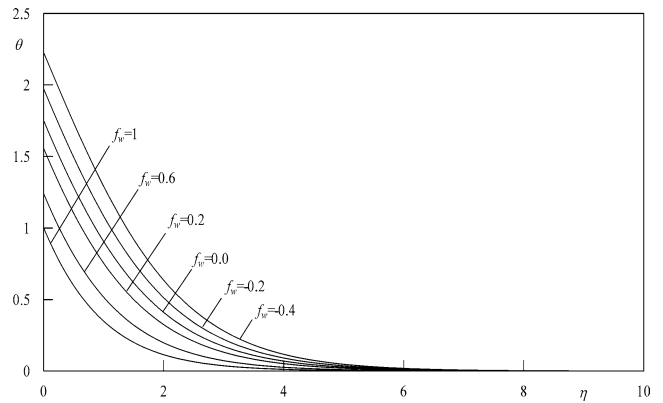


Fig. 19. Temperature profiles for various values of f_w with $M = 0.1$, $A^* = 0.01$, $m = 0.0$, $p = 0.5$, $\zeta = 0.5$ and $Pr = 0.7$, PHF case.

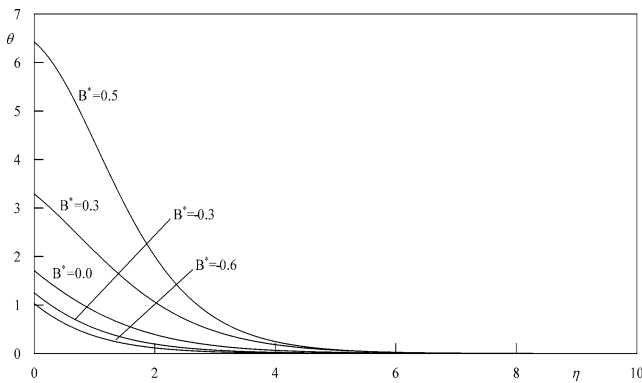


Fig. 17. Temperature profiles for various values of B^* with $M = 0.1$, $A^* = 0.01$, $f_w = 0$, $m = 0.0$, $p = 0.5$, $\zeta = 0.5$ and $Pr = 0.7$, PHF case.

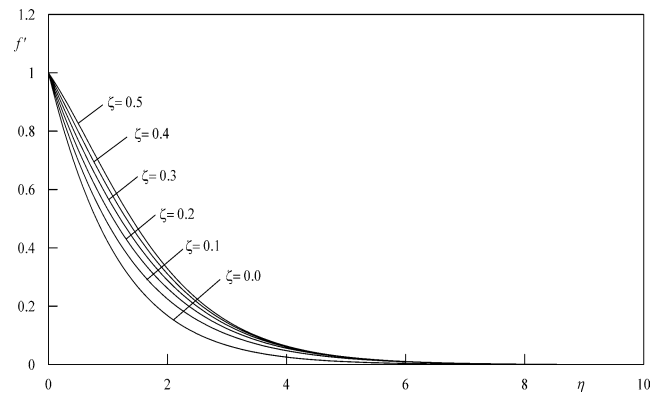


Fig. 20. Velocity profiles for various values of ζ with $M = 0.1$, $A^* = 0.01$, $B^* = 0.01$, $f_w = 0$, $p = 0.5$, $n = 0.5$ and $Pr = 0.7$, PHF case.

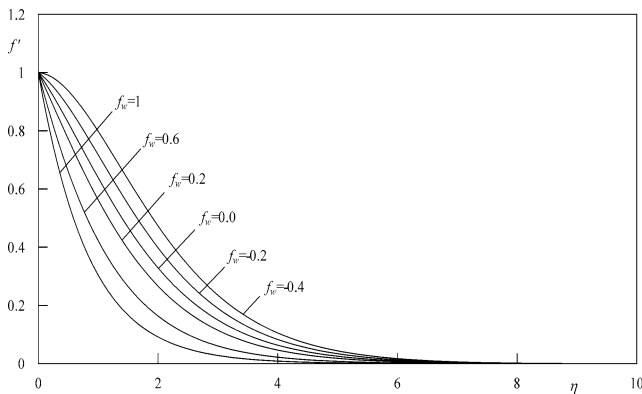


Fig. 18. Velocity profiles for various values of f_w with $M = 0.1$, $A^* = 0.01$, $m = 0.0$, $p = 0.5$, $\zeta = 0.5$ and $Pr = 0.7$, PHF case.

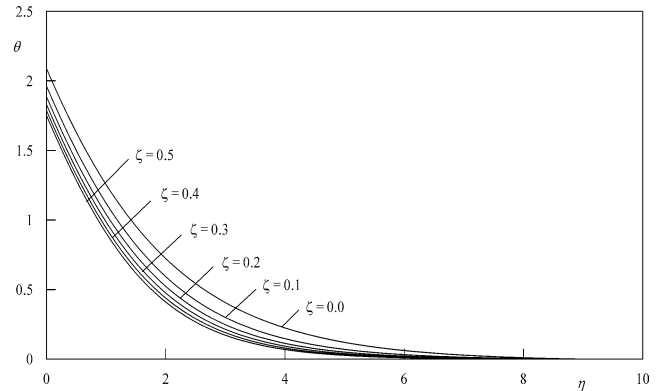


Fig. 21. Temperature profiles for various values of ζ with $M = 0.1$, $A^* = 0.01$, $B^* = 0.01$, $f_w = 0$, $p = 0.5$, $n = 0.5$ and $Pr = 0.7$, PHF case.

jection. The dimensionless wall shear stress $C_{f_x} Re_x^{1/2}$ decreases with increasing suction and increases with increasing injection. Figs. 10 and 11 are aimed to explore the effect of the buoyancy force parameter ξ on the velocity and temperature profiles. It is noticed that the velocity increases while the temperature decreases as the buoyancy force parameter ξ increases. Moreover, numerical results in Table 5 show that the local Nusselt number $Nu_x Re_x^{-1/2}$ and the local friction coefficient $C_{f_x} Re_x^{1/2}$ are both increased with in-

creasing ξ . This is due to the fact that positive ξ induces a favorable pressure gradient that enhances the fluid flow and heat transfer in the boundary layer. Figs. 12–21 are the graphical representation of the velocity and temperature profiles in PHF case for the same physical parameters used in Figs. 2–11 in PST case. Effects of all parameters on the flow and thermal fields are noticed to be similar but with markedly increased magnitude as compared to the PST case. From Figs. 14 and 16 it is clear that, there exist an over-

shooting of the velocity over the moving speed of the plate for higher values of A^* and B^* (e.g., $A^* = 1$ and $B^* = 0.5$). This velocity overshoot is due to the simultaneous effect of the internal heat generation and the heat flux which induce more flow due to the buoyancy effect as discussed before. Furthermore, it is observed from Figs. 15 and 17 that the temperature of the sheet is greatly increased for higher values of A^* and B^* . Values of $C_{fx}Re_x^{1/2}$ and $Nu_xRe_x^{-1/2}$ in PHF case for $Pr = 0.7$, $m = 0$ and $p = 0.5$ and various values of M , f_w , A^* , B^* and ζ are listed in Table 6. Numerical values indicate that both $C_{fx}Re_x^{1/2}$ and $Nu_xRe_x^{-1/2}$ increase as the magnetic field parameter M and the buoyancy force parameter ζ increase. From Tables 5 and 6 it is interesting to note that, for forced convection flow ($\xi = 0$ in PST case and $\zeta = 0$ in PHF case), the local friction coefficient $C_{fx}Re_x^{1/2}$ has the same value in both two cases. This result can be verified from the momentum equations for these two cases, Eqs. (7) and (16), that they can be brought into the same form and subject to the same boundary conditions when buoyancy force is neglected. Also, it is found that the local friction coefficient $C_{fx}Re_x^{1/2}$ increases while the local Nusselt number $Nu_xRe_x^{-1/2}$ decreases with increasing any of the following: injection parameter ($f_w < 0$), space-dependent heat source parameter ($A^* > 0$) and temperature-dependent heat source parameter ($B^* > 0$). On the other hand, local friction coefficient $C_{fx}Re_x^{1/2}$ decreases while the local Nusselt number $Nu_xRe_x^{-1/2}$ increases with increasing any of the following: suction parameter ($f_w > 0$), space-dependent heat source parameter ($A^* < 0$) and temperature-dependent heat source parameter ($B^* < 0$). The positive values of $C_{fx}Re_x^{1/2}$ is due to the distinctive peak in the velocity profiles caused by large values of A^* and B^* as seen earlier from Figs. 14 and 16.

4. Conclusion

The problem of steady laminar, hydromagnetic heat transfer by mixed convection adjacent to an inclined, permeable, continuously stretching sheet with power-law surface velocity in the presence of magnetic, heat generation/absorption which is a function of both space and temperature is investigated. The plate is maintained at prescribed surface temperature (PST) or prescribed heat flux (PHF). The governing equations for the flow are obtained by using suitable transformation and are solved numerically. Numerical results for the velocity and temperature profiles are presented graphically for various parametric conditions. In addition, Numerical data for the local skin-friction coefficient and the local Nusselt number are tabulated for various values of magnetic field parameter, coefficients of space-dependent and time-dependent internal heat generation/absorption, suction/blowing parameter and the buoyancy force parameters. It is found in both PST and PHF cases that:

- (1) The local friction coefficient and the local Nusselt number are depressed by rising M values, i.e., reduced as magnetic field strength increases.
- (2) The local Nusselt number decreases while the local friction coefficient increases as both space-dependent and time-dependent internal heat generation coefficients increase. The opposite impact was obtained as both space-dependent and time-dependent internal heat absorption coefficients increase.
- (3) Imposition of fluid wall suction increases the local Nusselt number and decreases the local friction coefficient. The opposite result was obtained as the fluid wall blowing was increased.
- (4) The local friction coefficient and the local Nusselt number are increased with increasing the value of the buoyancy force parameter.

References

- [1] B.C. Sakiadis, Amer. Inst. Chem. Engrg. J. 7 (1961) 26.
- [2] B.C. Sakiadis, Amer. Inst. Chem. Engrg. J. 7 (1961) 221.
- [3] L.E. Erickson, L.T. Fan, V.G. Fox, Indust. Engrg. Chem. Fund. 5 (1966) 19.
- [4] F.K. Tsou, E.M. Sparrow, R.J. Goldstien, Internat. J. Heat Mass Transfer 10 (1967) 219.
- [5] V.M. Soundalgekar, T.V. Ramana Murthy, Wärme-rund- Stoffübertragung 14 (1980) 91.
- [6] M.V. Karwe, Y. Jaluria, ASME J. Heat Transfer 110 (1988) 655.
- [7] D.B. Ingham, J. Applied Math. Phys. 37 (1986) 559.
- [8] M. Ali, F. Al-Yousef, Heat Mass Transfer 33 (1998) 310.
- [9] C.-H. Chen, Heat Mass Transfer 33 (1998) 471.
- [10] J.E. Danberg, K.S. Fansber, Quart. Appl. Math. 34 (1976) 305.
- [11] J. Veleggaar, Chem. Engrg. Sci. 32 (1977) 1517.
- [12] L.J. Grubka, K.M. Bobba, ASME J. Heat Transfer 107 (1985) 248.
- [13] M.E. Ali, Wärme-rund-Stoffübertragung 29 (1994) 227.
- [14] W.H.H. Banks, J. Mech. Theor. Appl. 2 (1983) 375.
- [15] M.E. Ali, Internat. J. Heat Fluid Flow 16 (1995) 280.
- [16] E.M.A. Elbashareshy, J. Phys. D Appl. Phys. 31 (1998) 1951.
- [17] K. Vajravelu, A. Hadjinalaou, Internat. J. Engrg. Sci. 35 (1997) 1237.
- [18] A. Chakrabarti, A.S. Gupta, Quart. Appl. Math. 37 (1979) 73.
- [19] T.C. Chiam, Internat. J. Engrg. Sci. 33 (1995) 429.
- [20] P. Chandran, N.C. Sacheti, A.K. Singh, Internat. Comm. Heat Mass Transfer 23 (1996) 889.
- [21] M. Subhas Abel, A. Joshi, R.M. Sonth, Z. Angew. Math. Mech. 81 (10) (2001) 691.
- [22] K. Vajravelu, J. Nayfeh, Internat. Comm. Heat Mass Transfer 19 (1992) 701.
- [23] K. Vajravelu, A. Hadjinalaou, Internat. Comm. Heat Mass Transfer 20 (1993) 417.
- [24] J.C. Crepeau, R. Clarksean, J. Heat Transfer 119 (1997) 183.
- [25] M. Subhas Abel, Sujit Kumar Khan, K.V. Prasad, Internat. J. Nonlinear Mech. 37 (2002) 81.
- [26] E.M. Abo-Eldahab, M.S. El Gendy, Phys. Scripta 62 (2000) 321.
- [27] E.M. Abo-Eldahab, Canad. J. Phys. 79 (2001) 1.
- [28] A.M. Jacobi, J. Heat Transfer 115 (1993) 1058.
- [29] P.S. Gupta, A.S. Gupta, Canad. J. Chem. Engrg. 55 (1977) 744.
- [30] K.N. Lashmishka, S. Venkateswaran, G. Nath, J. Heat Transfer 110 (1988) 590.